nature photonics

REVIEW ARTICLE

PUBLISHED ONLINE: 29 JANUARY 2010 | DOI: 10.1038/NPHOTON.2009.282

Plasmonics beyond the diffraction limit

Dmitri K. Gramotnev[1]* and Sergey I. Bozhevolnyi[2]*

Recent years have seen a rapid expansion of research into nanophotonics based on surface plasmon–polaritons. These electromagnetic waves propagate along metal–dielectric interfaces and can be guided by metallic nanostructures beyond the diffraction limit. This remarkable capability has unique prospects for the design of highly integrated photonic signal-processing systems, nanoresolution optical imaging techniques and sensors. This Review summarizes the basic principles and major achievements of plasmon guiding, and details the current state-of-the-art in subwavelength plasmonic waveguides, passive and active nanoplasmonic components for the generation, manipulation and detection of radiation, and configurations for the nanofocusing of light. Potential future developments and applications of nanophotonic devices and circuits are also discussed, such as in optical signals processing, nanoscale optical devices and near-field microscopy with nanoscale resolution.

The performance, speed and ease-of-use of semiconductor devices, circuits and components is dependent on their miniaturization and integration into external devices. However, the integration of modern electronic devices for information processing and sensing is rapidly approaching its fundamental speed and bandwidth limitations, which is an increasingly serious problem that impedes further advances in many areas of modern science and technology. One of the most promising solutions is believed to be in replacing electronic signals (as information carriers) by light. However, a major problem with using electromagnetic waves as information carriers in optical signal-processing devices and integrated circuits is the low levels of integration and miniaturization available, which are far poorer than those achievable in modern electronics. This problem is a consequence of the diffraction limit of light in dielectric media, which does not allow the localization of electromagnetic waves into nanoscale regions much smaller than the wavelength of light in the material[1].

The use of materials with negative dielectric permittivity is one of the most feasible ways of circumventing the diffraction limit and achieving localization of electromagnetic energy (at optical frequencies) into nanoscale regions as small as a few nanometres. The most readily available materials for this purpose are metals below the plasma frequency. Metal structures and interfaces are known to guide surface plasmon–polariton (SPP) modes[2], electromagnetic waves coupled to collective oscillations of electron plasma in the metal. As a result, plasmonics is an area of nanophotonics beyond the diffraction limit that studies the propagation, localization and guidance of strongly localized SPP modes using metallic nanostructures. The recent rapid development of plasmonic waveguides whose mode confinement is not limited by the material parameters of the guiding structure has been primarily driven by the tantalizing prospect of combining the compactness of an electronic circuit with the bandwidth of a photonic network.

Radiation guiding beyond the diffraction limit

The existence of surface plasmon–polariton waves, which are localized near and propagate along the interface of a plasma-like medium, has been known for decades[2]. However, the 'second birth' of SPPs and the recent rapid development of research in this area[3–5] occurred when scientists realized that SPP modes in metallic nanostructures may lead to the localization of guided light signals far beyond the diffraction limit for electromagnetic waves in dielectric media. This allows visible and infrared light to be concentrated into regions as small as a few nanometres, limited only by the atomic structure of matter, dissipation and the spatial dispersion of light[6,7]. The beginning of this major renewed interest in SPPs — particularly in SPP modes not subject to the diffraction limit — is marked by two papers published in 1997. The first demonstrated the possibility of subdiffraction guiding SPP modes in cylindrical metal nanowire or nanohole configurations[8], and the second introduced the idea of nanofocusing (that is, concentrating light energy into nanoscale regions) using SPP modes in wedge-like metallic structures[9]. These papers laid the foundation for one of the major research areas of modern plasmonics — SPP-based waveguides with subwavelength localization. This research has applications in the development of a new generation of nanophotonics devices and circuits, and as a means of concentrating and delivering light energy to nanoscale regions.

Plasmon nanoguiding. Various types of metallic nanostructure have been proposed for guiding SPP modes. These include thin metal films[10,11], chains of metal nanoparticles[12,13], cylindrical metal nanorods and nanoholes in a metallic medium[8,14], metal nanostrips on a dielectric substrate[15–19], nanogaps between metallic media[10,20–22], slot waveguides in the form of rectangular nanogaps in thin metal films[23–26], sharp metal wedges[27–31], nanogrooves in metal substrates[30–35] and hybrid plasmonic waveguides formed by dielectric nanowires coupled to a metal surface[36]. It is important to note that not all SPP modes guided by these structures can be used for achieving subwavelength localization of the guided signals. For example, metal films[10,11] and strips[15–19] can guide either long- or short-range SPPs, and decreasing the thickness of the film or strip results in poorer localization of the long-range mode. These long-range SPP modes experience only weak dissipation because only a small portion of the wave's energy is carried in the dissipative metal. Hence, they can propagate relatively large distances (of the order of millimetres at telecommunications frequencies), but do not exhibit subwavelength field localization, making them impossible to use in highly integrated optical circuits. In contrast, short-range SPP modes increase their localization with decreasing lateral dimensions of the guiding strip[15–19] (similar to metal nanorods; Fig. B1b). Although such modes are characterized by relatively strong dissipation and significantly smaller propagation distances than long-range SPP modes, their major advantage is the possibility of strong

[1]Nanophotonics, GPO Box 786, Brisbane, Queensland 4035, Australia. [2]Institute of Sensors, Signals and Electrotechnics (SENSE), University of Southern Denmark, Niels Bohrs Allé 1, DK-5230 Odense M, Denmark. *e-mail: d.gramotnev@nanophotonics.com.au; seib@sense.sdu.dk

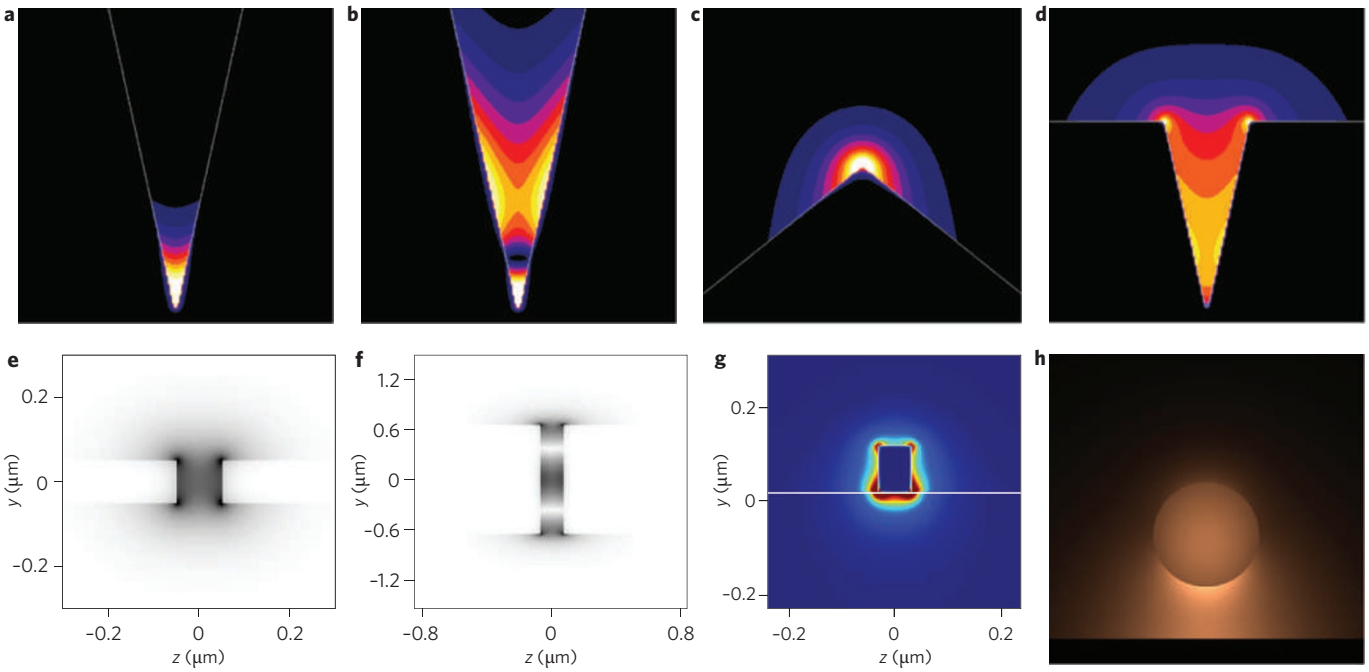

Figure 1 | Typical field distributions of guided strongly localized modes in various subwavelength plasmonic waveguides. a, Fundamental CPP mode in an infinitely deep metallic V-groove[30]. **b**, First higher CPP mode in an infinitely deep V-groove[30]. **c**, Fundamental wedge mode[28,30]. **d**, Fundamental CPP mode hybridized with wedge plasmons in a 1.172 μm groove in gold at the vacuum wavelength λ_{vac} = 1 μm (refs 30,34). **e**, Fundamental mode (formed by four wedge plasmons) in a slot in a silver membrane at λ_{vac} = 632.8 nm (refs 24–26). **f**, One of the higher modes of a slot waveguide in a silver membrane thicker than in (**e**), at λ_{vac} = 632.8 nm (refs 23,25,26). **g**, Fundamental mode in a gold nanostrip on a sapphire substrate (y < 0) at λ_{vac} = 1.48 μm (ref. 18). **h**, Hybrid mode of a GaAs nanowire in the glass host coupled to the silver surface at λ_{vac} = 1.55 μm (ref. 36). The diameter of the wire is 200 nm, and the separation between the wire and the silver substrate is 100 nm. Figures reproduced with permission from: **a**–**d**, ref. 30, © 2006 OSA; **e**,**f**, ref. 25, © 2005 AIP; **g**, ref. 18, © 2008 OSA; **h**, ref. 36, © 2008 NPG.

subwavelength localization of the guided signal — this is one of the major requirements for interconnects in highly integrated optical circuits and subwavelength optical devices and techniques (Box 1). This Review therefore focuses on short-range SPP modes guided by metallic nanostructures.

Not all of the previously analysed plasmonic waveguides are equally capable of guiding subwavelength plasmonic signals. For example, chains of nanoparticles exhibit very strong dissipation[13], which makes them difficult to use for efficient plasmonic interconnects. Nanoholes in a metallic medium are difficult to fabricate and also exhibit high dissipative losses[8,14]. Cylindrical nanowires may be sensitive to structural imperfections (for example, surface roughness and shape non-uniformities), and may also be difficult to fabricate and integrate into planar technology and nanocircuits. Metal strips and wedges are relatively easy to fabricate but are expected to exhibit relatively large bend losses and may be sensitive to structural imperfections. The detailed analysis of the actual impact of these factors on wedge plasmon waveguides and nanostrips is still to be investigated in detail.

At telecommunications frequencies (~1,300–1,550 nm), wedge plasmon waveguides have been shown to be superior to groove waveguide structures because of their strong subwavelength localization of guided plasmonic signals, relatively low dissipation and large propagation distances (hundreds of micrometres)[29,30,37]. This suggests that wedge plasmon waveguides are preferred[30,37] over V-groove waveguides[33–35] for subwavelength interconnects in the near-infrared. At optical frequencies, however, the situation is reversed; V-groove plasmonic waveguides provide stronger field localization and larger propagation distances[31,33,34] than metal wedges[28].

Typical field distributions of channel plasmon–polariton (CPP) modes and wedge plasmons guided by metallic V-grooves[30–35] and wedges[27–31] are shown in Figs 1a–d. In particular, it has been demonstrated that mode localization can be controlled by changing the taper angle of the V-groove or wedge: a smaller taper angle increases the localization of the guided modes and therefore increases the number of such SPP modes guided by these structures.

The existence conditions for CPP modes and wedge plasmons (including the typical acceptable ranges of the taper angles for the guiding grooves and wedges) have been derived and discussed[28,30,33–35,38,39]. The taper angles at which guided SPP modes exist in metal V-grooves and wedges, have strong subwavelength localization and propagate significant distances (around tens of micrometres for visible wavelengths) typically range from 10° to 90°. Furthermore, to effectively guide a CPP mode, the depth of a V-groove should not be significantly smaller than the penetration depth of the fundamental mode up the groove, which depends on the frequency, type of metal comprising the groove, the groove angle and dielectric filling the groove. For example, a depth of ~300 nm is required for a 30° vacuum V-groove in silver at λ_{vac} = 632.8 nm (ref. 34), and ~1 μm for a 25° vacuum V-groove in gold at λ_{vac} ~ 1 μm (ref. 30).

Experimental investigations have been conducted for both grooves[35,40,41] and wedges[29] at telecommunications frequencies, and for wedges at optical frequencies[28]. In particular, large propagation distances (up to hundreds of micrometres) at telecommunications wavelengths have been demonstrated, as well as strong subwavelength localization of the guided SPP modes.

Another important subwavelength plasmonic waveguide with characteristics similar to those of a V-groove waveguide is a nanoslot in a thin metal film or membrane[22–26]. Slot waveguides can support two different types of guided plasmonic eigenmodes[25,26]. The first type (including the fundamental mode; Fig. 1e) are formed by the propagation of coupled wedge plasmons along the four edges of the guiding rectangular slot[24–26]. The localization of this mode quickly increases (that is, it becomes more confined) and

Box 1 | Subwavelength guiding

Dielectric fibres and slabs can guide electromagnetic modes. Decreasing the diameter of a fibre (or the thickness of a slab) reduces the number of supported guided modes. The fundamental mode in an optical fibre/slab is the only mode with no cut-off diameter or thickness; when the fibre diameter d is decreased, the fundamental guided mode penetrates deeper into the surrounding medium and eventually (at $d = 0$) becomes a bulk plane-wave in the medium surrounding the fibre (Fig. B1a). At the same time, as $d \to 0$, the wavelength λ of the guided mode monotonically increases from λ_0, the wavelength of the bulk wave in the fibre medium (as $d \to \infty$), to the wavelength in the surrounding medium. As a result, the mode size (shown in Fig. B1a by the dashed lines) decreases when the diameter of the fibre is decreased to ~λ_0, and then increases to infinity when the fibre diameter is reduced further. Thus, decreasing the diameter of an optical fibre or the thickness of a guiding slab to zero cannot lead to subwavelength localization of the guided mode. This feature indicates the diffraction limit of light in dielectric waveguides and constitutes the main hurdle in achieving higher degrees of miniaturization and integration of optical devices and interconnects.

The situation for guiding SPP modes in plasmonic metal nanowires and waveguides is drastically different. When the diameter d of a cylindrical metal nanowire is reduced below the wavelength λ_{0sp} of the SPP on the flat metal interface, the fundamental SPP mode (whose magnetic field has axial symmetry and is perpendicular to the nanowire axis) experiences a strong monotonic increase in localization and a significant reduction in its phase and group velocities[8,45]. As a result, the diameter of the guided SPP mode can be decreased to just a few nanometres, limited only by the increased dissipative losses, the atomic structure of matter and spatial dispersion[6,7,45]. This feature is the principle behind using plasmonic nanostructures as subwavelength optical devices and interconnects for highly integrated nano-optics circuits and components, as well as for the delivery of light to the nanoscale, including to nano-optical devices, quantum dots and individual molecules.

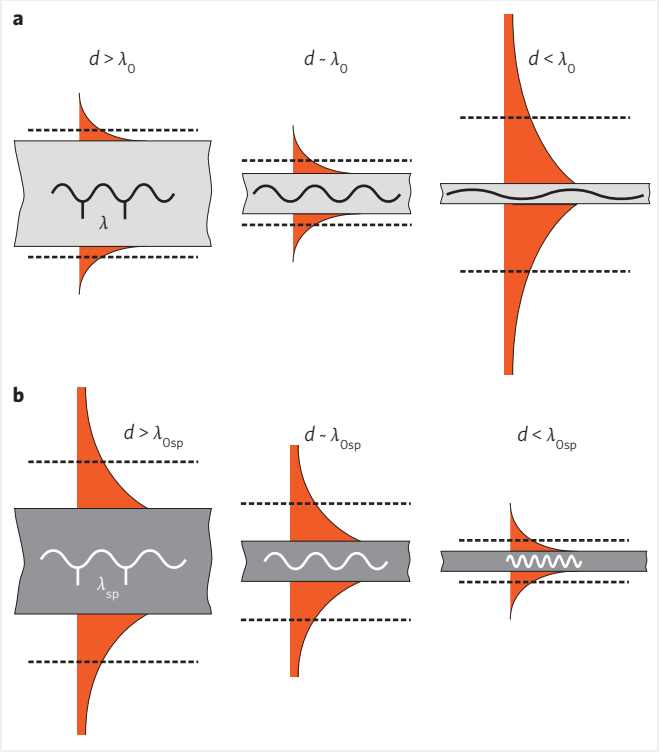

Figure B1 | Guided modes: dielectric fibres versus metal nanowires. **a**,**b**, Typical field structures, localization and wavelengths of the fundamental modes guided by dielectric fibres (**a**) and cylindrical metal nanowires (**b**) for different core diameters. λ_0 and λ_{0sp} are the mode wavelengths for infinite-diameter fibres or metal nanowires, respectively. The dashed horizontal lines show the localization of the mode at the 1/e level of the field.

its speed decreases as the thickness of the film and/or gap width is reduced[25,26]. The second type (Fig. 1f) are formed by a gap SPP experiencing successive reflections from the top and bottom of the slot[23,25,26]. The preliminary experimental observation of SPP modes in slot waveguides confirmed both their existence and significant propagation distances[25].

The possibility of coupling two neighbouring slot waveguides is important for the development of nanoscale directional couplers and for understanding how close two such waveguides can be placed together in a circuit before they begin to interfere with each other[23,42,43]. It has been shown that including additional metallic screening in the design of the slot waveguide could substantially reduce cross-talk without jeopardizing mode localization and propagation length[42].

Figures 1g and 1h present the typical field distributions in a metal nanostrip[18] and hybrid waveguide[36], respectively. In particular, Fig. 1g shows very strong subwavelength localization of the fundamental guided mode — more than 10 times smaller than $\lambda_{vac} \approx 1.48$ μm. A hybrid waveguide formed by a dielectric nanowire coupled to a metal surface (Fig. 1h) may also provide significant mode localization (particularly in the vertical direction) when the distance between the nanowire and the surface is reduced[36]. It also results in relatively low mode dissipation, and thus may significantly outperform other plasmonic guiding geometries in terms of the propagation length for comparable mode areas[36].

An understanding of the true advantages, efficiencies and optimization of different types of plasmonic/conventional waveguides and interconnects for integrated nano-optics and optical signal processing have been proposed and discussed[19,44]. These summaries consider the determined mode size, waveguide cross-talk, energy dissipation and three different numbers of merit, as well as giving important and useful methods of comparison.

Plasmon nanofocusing. One of the most tantalizing prospects of plasmonic subwavelength waveguides is their ability to concentrate (focus) light energy into nanoscale regions as small as a few nanometres. This plasmon nanofocusing[9,18,38,45–58] is typically achieved using tapered metallic guiding nanostructures such as tapered metal rods[45,46,52–54], sharp metal wedges[9,47,48,55], the tapered section of a metal film on a dielectric substrate[47], and the tapered nanogap between two metallic media[9,38,49–51,55].

Plasmon nanofocusing can occur in the adiabatic[38,45,47–49] and non-adiabatic[49–53] regime. In the adiabatic (or 'geometrical optics') approximation, the nanofocusing structure is weakly tapered (the taper angle is sufficiently small) so that the propagating SPP mode does not 'feel' the taper and thus does not experience any significant reflections from it. For example, at $\lambda_{vac} = 632.8$ nm in a gold tapered rod in vacuum, the adiabatic approximation is applicable up to taper angles of ~35° (ref. 53). If the taper angle is increased further, then significant reflections of the plasmon from the taper occur, which require rigorous numerical methods of analysis[49–53]. In this case, there exists an optimal taper angle for achieving maximum enhancement near the tip of the focusing structure[49–53], and also an optimal length of the taper[51,53].

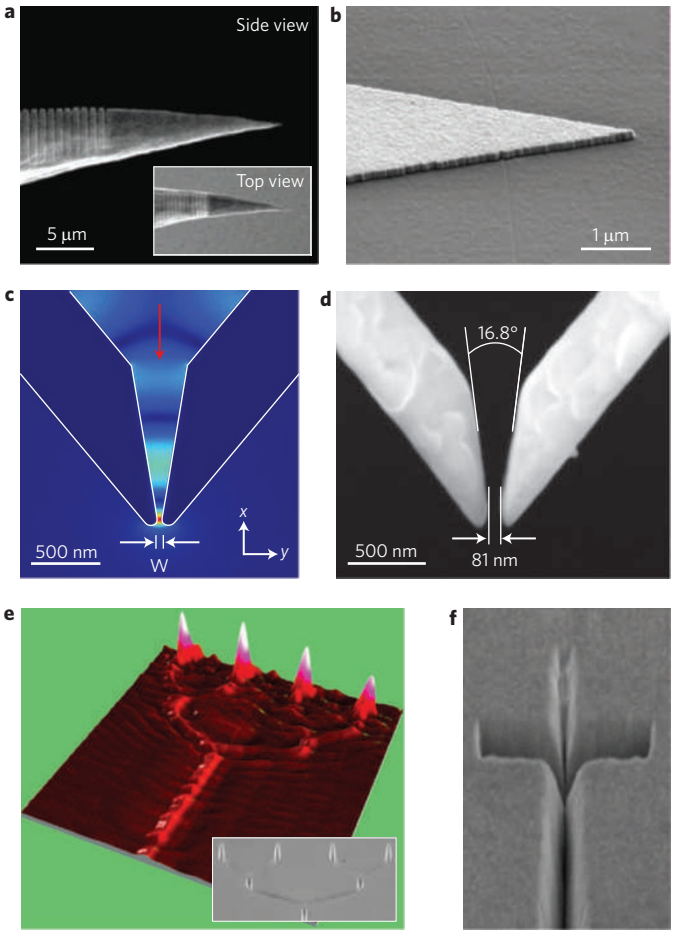

Figure 2 | Experimental structures for achieving plasmon nanofocusing. **a**, Tapered gold rod with a grating coupler for plasmon generation and nanofocusing at ~780–800 nm (ref. 56). **b**, A tapered section of a gold film on a sapphire substrate; the fundamental mode in the strip experiences nanofocusing near the tip of the taper[18]. **c**,**d**, Experimental realization of nanofocusing in tapered grooves, showing theoretical modelling of the plasmon coupling, propagation and enhancement in a fabricated tapered groove (**c**), and a scanning electron microscope (SEM) image of a typical V-groove cross-section (**d**). The groove has a wide upper region for 'catching' the incoming beam, and narrow lower region where nanofocusing takes place[57]. **e**, Near-field optical image (λ_{vac} = 1,500 nm) showing significant signal enhancements in the four groove tapers (a plasmonic 'candlestick') with gradually reduced depth and taper angle[58]. Inset, SEM image of 5-μm-long Y-splitters terminated by 2-μm-long tapers[58]. **f**, SEM image of a V-groove with the groove angle decreasing towards the taper end (top)[58]. Figures reproduced with permission from: **a**, ref. 56, © 2007 ACS; **b**, ref. 18, © 2008 OSA; **c**,**d**, ref. 57, © 2009 OSA; **e**–**g**, ref. 58, © 2009 ACS.

An interesting analytical approach based on the quasi-separation of variables and perturbation methods[54,55] has been developed as an alternative for plasmon nanofocusing in conical rods and wedge-like structures. This approach may allow determination of approximate analytical or semi-analytical plasmonic solutions in tapered metallic structures in the non-adiabatic regime.

So far, the strongest local field enhancement (up to ~2,000 times) for a nanofocusing structure has been predicted to be in tapered metal rods[53]. Wedges and tapered gaps may be less efficient in this respect, providing up to only ~10–100 times the local field enhancement with a tip of radius of a few nanometres[47,49–51]. All the nanofocusing structures considered above — except for wedges — provide equally strong field localization in regions as small as a few nanometres, limited only by spatial dispersion and the atomic structure of matter[6,7,45]. A single wedge typically provides slightly weaker localization in larger regions of ~10–20 nm. The local field enhancement in nanofocusing structures is heavily influenced by both the conditions at the tip and (in particular) the radius of the tip. For example, decreasing the tip radius from 10 nm to 2 nm for a tapered gold rod with a taper angle of ~35° (optimal for λ_{vac} = 632.8 nm) increases the local field enhancement at the tip from ~200 to ~1,600 times[53].

Several groups have reported successful observation of plasmon nanofocusing in a variety of metallic nanostructures[18,56–58]. For example, SPP modes were generated on the surface of a gold tapered rod using a grating coupler (Fig. 2a)[56]. Significant dipole radiation from the tip was observed, with the polarization and angular distribution confirming that it was generated by the strongly localized nanofocused transverse magnetic plasmon–polariton.

Plasmon nanofocusing in tapered gaps has been experimentally demonstrated and characterized at the wavelength of 1.53 μm (ref. 57). The fabricated structure used in this study (Fig. 2d) was a metallic groove with two tapered sections: ~70.6° (the input section for direct coupling of the incident light into the groove) and ~17° (the lower output section where nanofocusing occurs). Far-field power measurements from each of the output sections allowed determination of the light intensity (and thus the field enhancement) at the narrowest section of the tapered gap[57]. As a result, plasmonic fields have been concentrated (nanofocused) into regions as small as ~λ_{vac}/40, with a typical local field enhancement of at least 10 (in terms of the enhancement of the electric field intensity at the narrowest part of the gap)[57].

In another approach (Fig. 2e,f), plasmon nanofocusing was realized using CPP modes that propagate along triangular grooves of gradually decreasing depth and angle[58]. In this case, the gradually increasing localization of the CPP mode is equivalent to the two-dimensional focusing of the wave, and this results in a significant local field enhancement along the taper (~90 times, measured for the amplitude squared with a 2-μm-long taper[58]). The relative simplicity of fabrication allows consideration of more complex nanofocusing structures such as Y-splitters, which can provide multiple enhanced outputs (as shown in the 'plasmonic candlestick'; Fig. 2e).

Passive plasmonic components

Realization of the tremendous potential of SPP-based nanophotonic circuits is dependent on resolving several serious issues, such as the efficient coupling to nanoscale waveguides and the implementation of functional components within the limitations imposed by inevitable SPP propagation losses[59].

Plasmon coupling. Efficient coupling of input radiation — either freely propagating from a laser source or delivered by an optical fibre into a nanoscale SPP waveguide — is a challenge because of significant mode mismatch. One might adopt a generic coupling strategy that uses tapered configurations similar to those developed for plasmon nanofocusing, provided that the appropriate SPP mode (to be focused) can be efficiently excited[60,61]. Various coupling approaches have been developed and exploited for different waveguiding geometries.

In the case of metal nanowires, possibly the simplest method is to focus a laser beam onto one end facet of a nanowire whose extremity scatters the incident radiation in all directions. If the incident radiation is polarized along the nanowire axis, the laser excites the SPP nanowire mode by providing an additional wave vector (momentum) to match that of the SPP mode[62–64]. A propagating mode reaching the other end of the nanowire is partially scattered into free space, allowing observation of the mode excitation. It has also been shown that no mode can be excited when the

radiation is focused on a smooth nanowire surface (away from its ends and defects) and/or when the incident radiation is polarized perpendicular to the nanowire axis, which demonstrates the importance of both phase (wave vector) and field matching. Similarly, waveguide excitation can be achieved using properly polarized radiation to illuminate nanoscale structural non-uniformities (such as defects, bends and junctions) in a waveguide, as well as nanoparticles placed close to a nanowire[64–66]. It was recently demonstrated that radiation can also be delivered to a nanowire end facet via a dielectric waveguide oriented perpendicular to the nanowire axis to provide the required mode polarization — the advantage being that several nanowires can be excited simultaneously[67].

Efficient excitation of a nanowire's fundamental SPP mode is a serious challenge. This is because of the field symmetry in this mode: one of the main electric field components is radially polarized, so the incident radiation, which is typically linearly polarized, can be coupled into the nanowire only through the longitudinal field component parallel to the nanowire axis. In contrast, the CPP field is mostly linearly polarized (perpendicular to the groove sides), which allows the use of straightforward and quite efficient end-fire excitation with a tapered polarization-maintaining single-mode fibre[35,40,41]. Finally, it should be noted that a coupling efficiency of up to ~70% was predicted to be feasible for the end-fire coupling between high-index contrast dielectric slab waveguides and gap SPP waveguides[68] (whose fundamental mode is similar to the CPP in terms of its polarization properties).

Plasmon routing and filtering. Realization of SPP-based nanophotonic components poses another difficult challenge because of laborious fabrication processes (for example, metal nanowires have so far been fabricated only chemically, which does not allow deterministic control over their topology[62–67]) and inevitable propagation losses that increase rapidly with decreasing plasmonic mode size. Note that mode shape and confinement determines both the bend loss and minimum waveguide separation, and therefore has a crucial role in the miniaturization of waveguide components[5]. For example, strongly confined gap SPPs were shown through numerical simulation[22] to be suitable for the design of nanoscale photonic circuits (formed by silver–air–silver gaps of varying width) for efficient multiport branching within an area smaller than λ_{vac}^2. Designs of nearly lossless 90° bends[69] and nanoscale Fabry–Pérot inteferometers[70] based on CPP waveguiding in silver V-grooves have also been suggested using numerical simulations (Fig. 3a,b). Mode propagation around sharp bends has been experimentally observed with both silver nanowires supporting cylindrical SPPs[64] and gold V-grooves guiding CPPs[40] (Fig. 3c,d). Furthermore, the enormous potential offered by subwavelength mode confinement has also been demonstrated using CPP-based waveguide components such as Mach–Zehnder interferometers and ring resonators[40], and also using add-drop multiplexers and Bragg gratings[41], which can be significantly smaller than plasmonic components based on diffraction-limited SPP waveguide configurations.

Another important aspect of subwavelength waveguiding using plasmons is the wavelength selectivity $\delta\lambda$, which is introduced by the loss. The expression $\delta\lambda/\lambda \sim 0.5\lambda_{sp}/L_{sp}$, where λ_{sp} is the SPP wavelength, shows that the wavelength selectivity decreases as the loss increases (that is, propagation length L_{sp} decreases). For example, a CPP-based ring resonator at telecommunications wavelengths (~1.5 μm) can be designed to work as a switch between the open (transmission) and closed (absorption) states when tuning the wavelength by ~22.5 nm, provided that the ring circumference L_{sp} is ~50 μm. It has indeed been demonstrated[71] that a 10-μm-radius ring resonator exhibits switching between the two transmission states when the wavelength is tuned over ~20 nm (Fig. 4).

Plasmonic nano-antennas. The underlying physics of the SPP-based nanophotonic components considered above is extremely important for the design and realization of nano-antennas and resonators, which constitute an example of stand-alone plasmonic components and could also be integrated in nanophotonic circuits to facilitate plasmon coupling and detection. The main idea[72] is to exploit retardation-based resonances involving short-range SPP modes, which, owing to their nanoscale confinement, can be efficiently reflected by terminations in a waveguiding nanostructure (such as a stripe[72], metal–dielectric–metal gap[73] or wire[74]). Such a nanostructure therefore functions as a Fabry–Pérot cavity with a resonance condition $L(2\pi/\lambda_{sp}) = m\pi - \varphi$ (where L is the nanostructure length and φ is the reflection phase). Depending on the particular SPP mode symmetry, a finite-length nanostructure at resonance can have a field distribution similar to that of an electric (stripe or wire) or magnetic (gap) dipole, and correspondingly strong scattering (similar to that of an antenna) or resonating properties[75]. In either case, because the short-range SPP wavelength tends to zero when the structure width decreases, one can design nano-antennas and resonators with dimensions as small as a few nanometres (limited only by the atomic structure of matter and spatial dispersion[6,7,45]), which operate at any given wavelength[72–75]. Experimentally, optical resonances in individual metal nanowires[63,76–78], gap cavities[73,79] and nanostrip[80] antennas have been successfully observed and attributed to the occurrence of a standing-wave pattern formed by counter-propagating SPP modes. The importance of accurately taking into account the phase change φ accumulated on reflection by the structure termination has also been demonstrated[79–81]. A properly designed plasmonic nano-antenna with a gap in which the local field is strongly enhanced (owing to the boundary conditions)[72] can be advantageously used to concentrate and detect radiation in nanoscale volumes, thereby providing a new method for ultrafast detection[82].

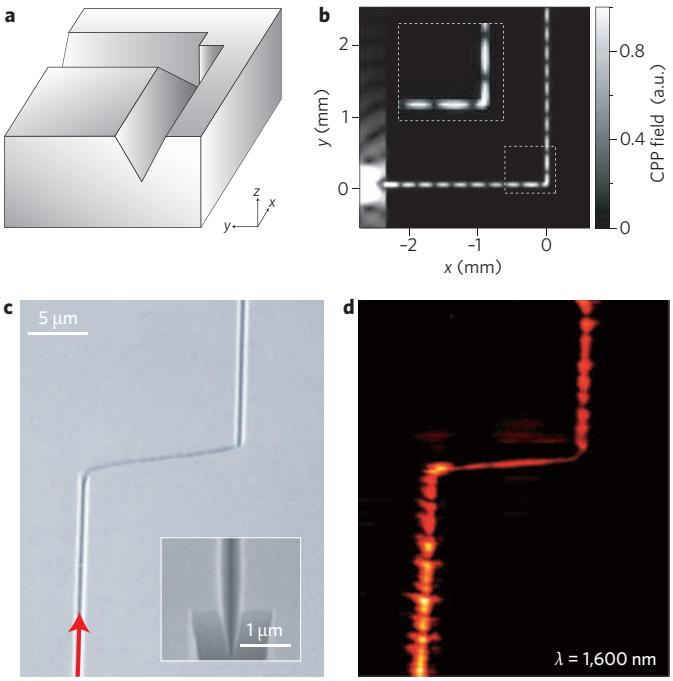

Figure 3 | Plasmon guiding around sharp bends. a, V-groove subwavelength waveguide structure with a sharp 90° bend. **b**, Top-down view of the calculated CPP field distribution at a distance of 60 nm from the bottom of a V-groove in silver. The groove angle is 30° and the wavelength is 633 nm. **c**,**d**, A sharply bent (smallest radius of curvature of 0.83 μm) V-groove in gold, showing an electron microscope image with the groove profile inset (**c**), and a near-field optical image at λ_{vac} = 1,600 nm (**d**). Figures reproduced with permission from: **a**,**b**, ref. 69, © 2005 OSA; **c**,**d**, ref. 116, © 2006 AIP.

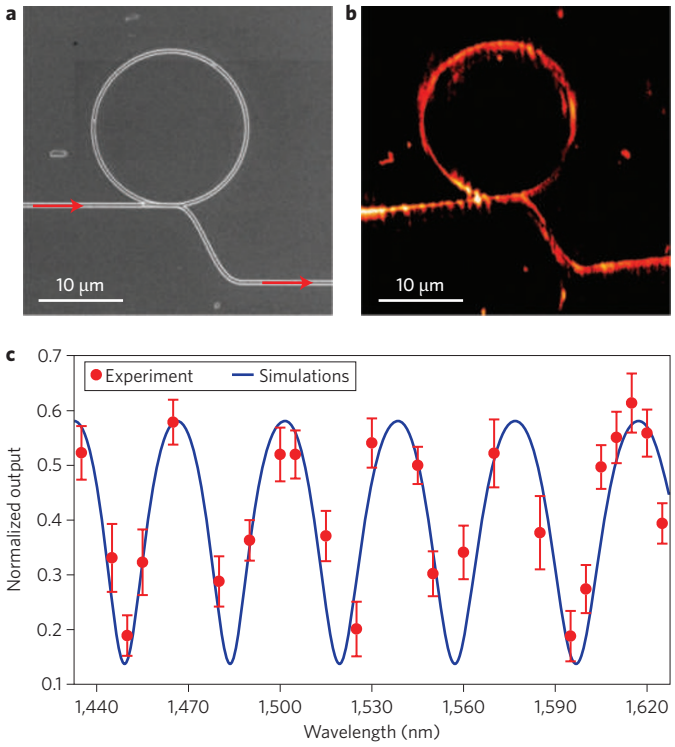

Figure 4 | Plasmonic waveguide-ring resonator. a,**b**, 10-μm-radius waveguide-ring resonator, showing an SEM image (**a**), and a near-field optical image at λ_{vac} = 1,500 nm (**b**). **c**, Transmission waveguide-ring resonator spectra determined experimentally from near-field optical images (similar to **b**) and using an analytical fit. The error bars are estimated from the maximum variation of the normalized output for different positions along the input and output channels.

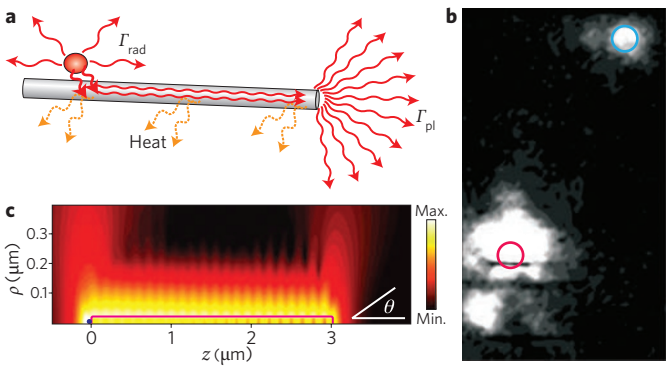

Figure 5 | Generation of optical plasmons using a quantum dot placed near a silver nanowire. a, Quantum dot emission channels, showing plasmon propagation, dissipation and radiation. Γ_{rad} and Γ_{pl} are the spontaneous emission rates into bulk waves and SPP modes, respectively. **b**, Fluorescence microscope image showing the excited quantum dot (red circle) near a silver nanowire (not visible) whose ends radiate excited plasmons (blue circle). **c**, Simulation of the electric field amplitude emitted by a dipole (blue dot) positioned 25 nm from one end of a 3-μm-long, 50-nm-diameter silver nanowire (surface outlined). The vertical scale (ρ) is enlarged compared with the horizontal (z) to clearly show the near-field of the surface plasmons. When the plasmons reach the far end of the nanowire, some are clearly scattered to the far-field, while the remaining ones are either lost to dissipation or to back-reflection. Figures reproduced with permission from ref. 106, © 2007 NPG.

Active nanoplasmonics

To be complete, plasmonic circuits will have to incorporate active components that can generate suitable SPP modes, modulate the transmitted field phase and/or amplitude, and detect output radiation, preferably without converting SPP modes into freely propagating light waves.

Plasmon modulation. Implementation of field modulation in an SPP waveguide configuration is strongly influenced by its material composition and the strength of material effects available, such as thermo-, electro- and magneto-optical effects or optical nonlinearities (for all-optical radiation control). However, because all of these effects are inherently weak and the propagation distances of nanoscale-confined SPP modes are very small, the challenge of realizing SPP modulation is enormous. Long-range SPP-based thermo-optical modulators and switches were the first plasmonic components in which the same metal circuitry was used to both guide the optical radiation and transmit the electrical signals that efficiently control the guidance[83]. In early attempts to exploit SPPs for light modulation, the main operation principle was to perturb the attenuated total reflection, for example by piezo-electrically varying the prism–metal gap[84], which is efficient (~75%) but slow (~100 kHz), or by electro-optically changing the refractive index of the polymer film adjacent to the metal[85], which is extremely fast (~20 GHz) but inefficient (~0.1%). Both configurations are bulky and difficult to downscale.

Recently, electro-optical modulation in thin-film interferometers that support SPP propagation (along an interface between silver and barium titanate[86]) and the electrical control of light transmission using a field-effect silicon modulator based on multimode interference in a plasmonic waveguide[87] were realized using planar components. However, in terms of operation speed, all-optical control has the potential for the fastest switching. A much larger dynamic range of light absorption in plasmonic structures, compared with that of the real part of the refractive index, opens the possibility for efficient all-optical modulation of SPP transmission by influencing absorption in the metal[88] and dielectric (using quantum dots[89] and photochromic molecules[90]). This has allowed femtosecond switching to be reached[88–90]. It should be noted that, in the above examples[84–90], the modulation was achieved using planar SPP modes (that is, not confined in the lateral direction), so the challenge of modulating guided localized SPP modes is also yet to be tackled.

Plasmon amplification, generation and detection. Some of the challenges mentioned above, such as the short-propagation distances for modes with strong field confinement, would be greatly alleviated if SPP propagation losses were significantly decreased. One way of compensating for SPP loss is to introduce optical gain in the dielectric material adjacent to a metal[91]. This is challenging, however, because the gain required to match the SPP dissipative loss is very large.

Generally, losses are smaller at longer wavelengths. As a result, SPP-based lasers have been successfully realized in the mid-infrared range — these are essentially semiconductor quantum cascade lasers with SPP waveguides[92,93]. A principle for offsetting SPP loss using gain was demonstrated for visible wavelengths only a few years ago[94], and very recently some SPP loss compensation was claimed for visible wavelengths using optically pumping dye-impregnated polymers[95], and for telecommunications wavelengths using erbium-doped phosphate glass[96] and polymers embedded with quantum dots[97]. Experiments using dye-impregnated polymers resulted in the observation of SPP stimulated emission, with efficient feedback being the only missing link to realize the generation of a coherent SPP beam[98]. Furthermore, direct polychromatic SPP excitation/generation has been demonstrated using free-electron irradiation of metal films[99,100] and organic red-emitting LEDs designed to allow SPP extraction[101].

The above configurations[91–101] exploit SPP modes that are only weakly confined (that is, diffraction limited) in width, thus helping to minimize propagation losses, which always rise with increasing mode confinement. However, strongly confined (nanoscale) SPP modes are ideally suited for efficient excitation by individual nano-emitters. Theoretical considerations of metal nanowires[102,103] and metal–dielectric–metal slot waveguides[104] have indicated that the corresponding SPP modes can be very strongly coupled to nearby emitters, resulting in the broadband (non-resonant) enhancement of spontaneous emission and the efficient generation of single optical plasmons. Experimentally, efficient exciton–plasmon–photon conversion at ~650 nm was demonstrated[105] (including at the single-photon level[106]) using CdSe quantum dots placed near to silver nanowires , with efficiencies of up to ~50% for a single CdSe quantum dot emitting into nanowire SPPs and single plasmons (Fig. 5). This remarkable achievement has many exciting prospects, such as the realization of single-photon transistors[107].

Realizing the enormous potential of the SPP-based nanophotonic components discussed above also requires efficient detection techniques that can be integrated directly into plasmonic circuits. The first steps in this direction were accomplished very recently, resulting in direct electrical detection of propagating SPP modes supported by planar air–metal[108] and metal–insulator–metal[109] structures, as well as by metal nanowires[110]. The SPP detection schemes were based on the SPP coupling to an organic diode[108], a nanoslit metal–semiconductor–metal photodetector[109] (Fig. 6a) and a nanowire field-effect transistor[110] (Fig. 6b), respectively. For the nanowire field-effect transistor, SPP generation by an individual quantum dot[106] was integrated with the electrical SPP detection, thus providing a complete plasmo-electronic nanocircuit.

Conclusions

The ongoing studies into plasmonic nanostructures capable of guiding surface plasmons beyond the diffraction limit have already demonstrated the unique capability of these structures for efficient concentration and manipulation of light in nanoscale regions. These structures have also demonstrated their ability to deliver light energy to nanoscale optical and electronic devices, quantum dots and even separate molecules. The possibility of strong subwavelength localization of guided plasmonic signals makes these structures particularly useful for the future design and development of highly integrated and efficient nano-optical signal-processing devices and circuits[59]. They are also expected to provide an essential and efficient link between conventional optical communication components and nano-electronic systems for data and information processing.

Plasmonic nanofocusing structures have demonstrated strong local field enhancement and confinement, which has potential for the design of new generations of sensors, detectors and nano-imaging techniques. Such techniques enable optical characterization of separate molecules. This may lead to new optical nanomanipulation methods in nanotechnology, biophotonics and medical testing. The unique features of plasmonic nanostructures are being intensively explored in other exciting directions of research, such as localized plasmon excitations in metal nanoparticles[111], plasmon-mediated enhanced optical transmission through subwavelength apertures[112] and heat-assisted magnetic recording using the near-field in plasmonic structures[113]. It is also important to note that due to the rapid development of active plasmonics, this Review may not adequately cover the most recent advances in this exciting area[114,115].

Important future practical applications of plasmon guiding structures in optical signal processing, sensing and imaging — including the realization of their unique features and benefits — are strongly dependent on further theoretical advances in this area. However, these future applications are even more dependent on the successful development of experimental methods and techniques for the reliable fabrication of optimally designed structures,

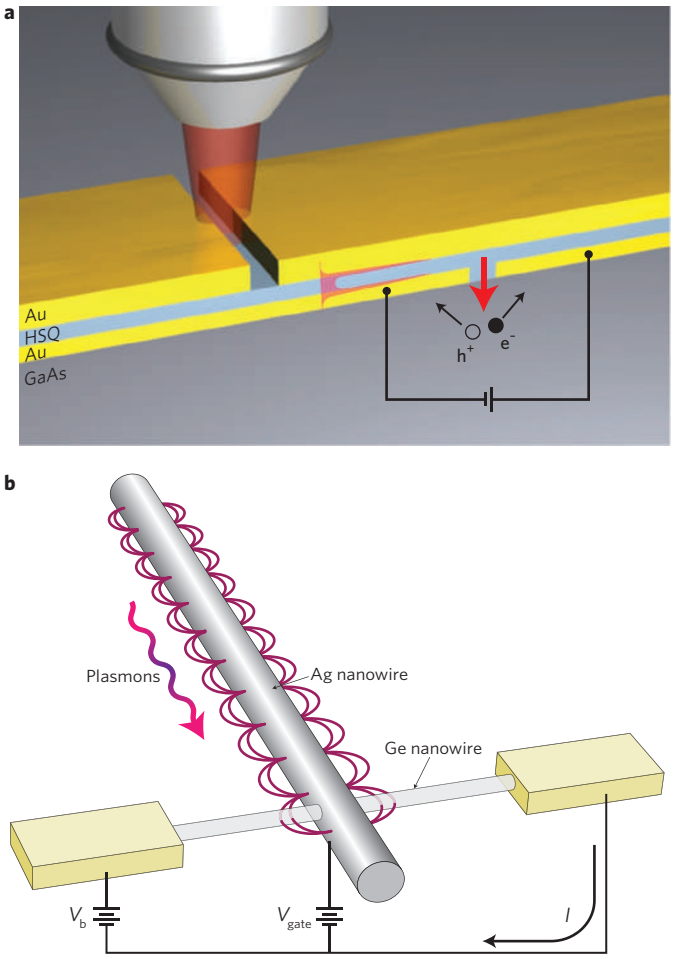

Figure 6 | Electrical detection of plasmons. a, Plasmon (far-field) excitation, propagation in a dielectric gap between metal films, and detection by a semiconductor. The plasmonic waveguide consists of a gold (100 nm)/hydrogen silsesquioxane (HSQ; 90 nm)/gold (160 nm) layer stack. **b**, Plasmon detection with a nanowire field-effect transistor using electron–hole pair generation and separation in the detector. V_b is the bias voltage. Figures reproduced with permission from: **a**, ref. 109, © 2009 NPG; **b**, ref. 110, © 2009 NPG.

the efficient generation of plasmonic modes guided beyond the diffraction limit, and the detection of signals from nanoscale objects (including single molecules). Plasmonics is still in its infancy, and the practical integration of all plasmonic components designed for efficient plasmon generation, manipulation and detection is a significant and formidable technological challenge.

References

1. Born, M. & Wolf, E. *Principles of Optics* 7th edn, Ch. 8 (Cambridge Univ. Press, 1999).
2. Raether, H. *Surface Plasmons on Smooth and Rough Surfaces and on Gratings*, Ch. 2 (Springer, 1988).
3. Maier, S. A. & Atwater, H. A. Plasmonics: Localization and guiding of electromagnetic energy in metal/dielectric structures. *J. Appl. Phys.* **98,** 011101 (2005).
4. Barnes, W. L. Surface plasmon–polariton length scales: A route to sub-wavelength optics. *J. Opt. A* **8,** S87–S93 (2006).
5. Ebbesen, T. W., Genet, C. & Bozhevolnyi, S. I. Surface-plasmon circuitry. *Phys. Today* **61,** 44–50 (May 2008).
6. Liebsch, A. Screening properties of a metal surface at low frequencies and finite wave vectors. *Phys. Rev. Lett.* **54,** 67–70 (1985).
7. Larkin, I. A., Stockman, M. I., Achermann, M. & Klimov, V. I. Dipolar emitters at nanoscale proximity of metal surfaces: Giant enhancement of relaxation in microscopic theory. *Phys. Rev B* **69,** 121403 (2004).

8. Takahara, J., Yamagishi, S., Taki, H., Morimoto, A. & Kobayashi, T. Guiding of a one-dimensional optical beam with nanometer diameter. *Opt. Lett.* **22,** 475–477 (1997).
9. Nerkararyan, K. V. Superfocusing of a surface polariton in a wedge-like structure. *Phys. Lett. A* **237,** 103–105 (1997).
10. Economou, E. N. Surface plasmons in thin films. *Phys. Rev.* **182,** 539–554 (1969).
11. Burke, J. J., Stegeman, G. I. & Tamir, T. Surface-polariton-like waves guided by thin, lossy metal films. *Phys. Rev B* **33,** 5186–5201 (1986).
12. Quinten, M., Leitner, A., Krenn, J. R. & Aussenegg, F. R. Electromagnetic energy transport via linear chains of silver nanoparticles. *Opt. Lett.* **23,** 1331–1333 (1998).
13. Maier, S. A. *et al.* Local detection of electromagnetic energy transport below the diffraction limit in metal nanoparticle plasmon waveguides. *Nature Mater.* **2,** 229–232 (2003).
14. Onuki, T. *et al.* Propagation of surface plasmon polariton in nanometre-sized metal-clad optical waveguides. *J. Microsc.* **210,** 284–287 (2003).
15. Berini, P. Plasmon-polariton waves guided by thin lossy metal films of finite width: Bound modes of asymmetric structures. *Phys Rev. B* **63,** 125417 (2001).**[AU: OK?].**
16. Krenn, J. R. *et al.* Non-diffraction-limited light transport by gold nanowires. *Europhys Lett.* **60,** 663–669 (2002).
17. Zia, R., Schuller, J. A. & Brongersma, M. L. Near-field characterization of guided polariton propagation and cutoff in surface plasmon waveguides. *Phys. Rev. B* **74,** 165415 (2006).
18. Verhagen, E., Polman, A. & Kuipers, L. K. Nanofocusing in laterally tapered plasmonic waveguides. *Opt. Express* **16,** 45–57 (2008).
19. Berini, P. Figures of merit for surface plasmon waveguides. *Opt. Express* **14,** 13030–13042 (2006).
20. Tanaka, K. & Tanaka, M. Simulations of nanometric optical circuits based on surface plasmon polariton gap waveguide. *Appl. Phys. Lett.* **82,** 1158–1160 (2003).
21. Wang, B. & Wang, G. P. Surface plasmon polariton propagation in nanoscale metal gap waveguides. *Opt. Lett.* **29,** 1992–1994 (2004).
22. Tanaka, K., Tanaka, M. & Sugiyama, T. Simulation of practical nanometric optical circuits based on surface plasmon polariton gap waveguides. *Opt. Express* **13,** 256–266 (2005).
23. Liu, L., Han, Z. & He, S. Novel surface plasmon waveguide for high integration. *Opt. Express* **13,** 6645–6650 (2005).
24. Veronis, G. & Fan, S. Guided subwavelength plasmonic mode supported by a slot in a thin metal film. *Opt. Lett.* **30,** 3359–3361 (2005).
25. Pile, D. F. P. *et al.* Two-dimensionally localized modes of a nanoscale gap plasmon waveguide. *Appl. Phys. Lett.* **87,** 261114 (2005).
26. Pile, D. F. P., Gramotnev, D. K., Oulton, R. F. & Zhang, X. On long-range plasmonic modes in metallic gaps. *Opt. Express* **15,** 13669–13674 (2007).
27. Boardman, A. D., Aers, G. C. & Teshima, R. Retarded edge modes of a parabolic wedge. *Phys. Rev. B* **24,** 5703–5712 (1981).
28. Pile, D. F. P. *et al.* Theoretical and experimental investigation of strongly localized plasmons on triangular metal wedges for subwavelength waveguiding. *Appl. Phys. Lett.* **87,** 061106 (2005).
29. Boltasseva, A. *et al.* Triangular metal wedges for subwavelength plasmon–polariton guiding at telecom wavelengths. *Opt. Express* **16,** 5252–5260 (2008).
30. Moreno, E., Garcia-Vidal, F. J., Rodrigo, S. G., Martin-Moreno, L. & Bozhevolnyi, S. I. Channel plasmon-polaritons: Modal shape, dispersion, and losses. *Opt. Lett.* **31,** 3447–3449 (2006).
31. Yan, M. & Qiu, M. Guided plasmon polariton at 2D metal corners. *J. Opt. Soc. Am. B* **24,** 2333–2342 (2007).
32. Novikov, I. V. & Maradudin, A. A. Channel polaritons. *Phys. Rev. B* **66,** 035403 (2002).
33. Pile, D. F. P. & Gramotnev, D. K. Channel plasmon–polariton in a triangular groove on a metal surface. *Opt. Lett.* **29,** 1069–1071 (2004).
34. Gramotnev, D. K. & Pile, D. F. P. Single-mode subwavelength waveguide with channel plasmon–polaritons in triangular grooves on a metal surface. *Appl. Phys. Lett.* **85,** 6323–6325 (2004).
35. Bozhevolyni, S. I., Volkov, V. S., Devaux, E. & Ebbesen, T. W. Channel plasmon–polariton guiding by subwavelength metal grooves. *Phys. Rev. Lett.* **95,** 046802 (2005).
36. Oulton, R. F., Sorger, V. J., Genov, D. A., Pile, D. F. P. & Zhang, X. A hybrid plasmonic waveguide for subwavelength confinement and long-range propagation. *Nature Photon.* **2,** 496–500 (2008).
37. Moreno, E., Rodrigo, S. G., Bozhevolnyi, S. I., Martín-Moreno, L. & García-Vidal, F. J. Guiding and focusing of electromagnetic fields with wedge plasmon polaritons. *Phys. Rev*. Lett. **100,** 023901 (2008).
38. Gramotnev, D. K. Adiabatic nanofocusing of plasmons by sharp metallic grooves: Geometrical optics approach. *J. Appl. Phys.* **98,** 104302 (2005).
39. Bozhevolnyi, S. I. & Nerkararyan, K. V. Analytic description of channel plasmon polaritons. *Opt. Lett.* **34,** 2039–2041 (2009).
40. Bozhevolnyi, S. I., Volkov, V. S., Devaux, E., Laluet, J.-Y. & Ebbesen, T. W. Channel plasmon subwavelength waveguide components including interferometers and ring resonators. *Nature* **440,** 508–511 (2006).
41. Volkov, V. S., Bozhevolnyi, S. I., Devaux, E., Laluet, J.-Y. & Ebbesen, T. W. Wavelength selective nanophotonic components utilizing channel plasmon polaritons. *Nano Lett.* **7,** 880–884 (2007).
42. Veronis, G. & Fan, S. Crosstalk between three-dimensional plasmonic slot waveguides. *Opt. Express* **16,** 2129–2140 (2008).
43. Gramotnev, D. K., Vernon, K. C. & Pile, D. F. P. Directional coupler using slot plasmonic waveguide. *Appl. Phys. B* **93,** 99–106 (2008).
44. Conway, J. A., Sahni, S. & Szkopek, T. Plasmonic interconnects versus conventional interconnects: A comparison of latency, crosstalk and energy costs. *Opt. Express* **15,** 4474–4484 (2007).
45. Stockman, M. I. Nanofocusing of optical energy in tapered plasmonic waveguides. *Phys. Rev. Lett.* **93,** 137404 (2004).
46. Babadjanyan, A. J., Margaryan, N. L. & Nerkararyan, K. V. Superfocusing of surface polaritons in the conical structure. *J. Appl. Phys.* **87,** 3785–3788 (2000).
47. Vernon, K. C., Gramotnev, D. K. & Pile, D. F. P. Adiabatic nanofocusing of plasmons by a sharp metal wedge on a dielectric substrate. *J. Appl. Phys.* **101,** 104312 (2007).
48. Durach, M., Rusina, A., Stockman, M. I. & Nelson, K. Toward full spatiotemporal control on the nanoscale. *Nano Lett.* **7,** 3145–3149 (2007).
49. Pile, D. F. P. & Gramotnev, D. K. Adiabatic and nonadiabatic nanofocusing of plasmons by tapered gap plasmon waveguides. *Appl. Phys. Lett.* **89,** 041111 (2006).
50. Ginzburg, P., Arbel, D. & Orenstein, M. Gap plasmon polariton structure for very efficient microscale-to-nanoscale interfacing. *Opt. Lett.* **31,** 3288–3290 (2006).
51. Gramotnev, D. K., Pile, D. F. P., Vogel, M. W. & Zhang, X. Local electric field enhancement during nanofocusing of plasmons by a tapered gap. *Phys. Rev. B* **75,** 035431 (2007).
52. Issa, N. A. & Guckenberger, R. Optical nanofocusing on tapered metallic waveguides. *Plasmonics* **2,** 31–37 (2007).
53. Gramotnev, D. K., Vogel, M. W. & Stockman, M. I. Optimized nonadiabatic nanofocusing of plasmons by tapered metal rods. *J. Appl. Phys.* **104,** 034311 (2008).
54. Kurihara, K. *et al.* Superfocusing modes of surface plasmon polaritons in conical geometry based on the quasi-separation of variables approach. *J. Phys. A* **40,** 12479–12503 (2007).
55. Kurihara, K., Yamamoto, K., Takahara, J. & Otomo, A. Superfocusing modes of surface plasmon polaritons in a wedge-shaped geometry obtained by quasi-separation of variables. *J. Phys. A* **41,** 295401–295500 (2008).
56. Ropers, C. *et al.* Grating-coupling of surface plasmons onto metallic tips: A nanoconfined light source. *Nano Lett.* **7,** 2784–2788 (2007).
57. Choi, H., Pile, D. F., Nam, S., Bartal, G. & Zhang, X. Compressing surface plasmons for nanoscale optical focusing. *Opt. Express* **17,** 7519–7524 (2009).
58. Volkov, V. S. *et al.* Nanofocusing with channel plasmon polaritons. *Nano Lett.* **9,** 1278–1282 (2009).
59. *Plasmonic Nanoguides and Circuits*, Bozhevolnyi S. I., ed. (Pan Stanford, 2009).
60. Chen, L., Shakya, J. & Lipson, M. Subwavelength confinement in an integrated metal slot waveguide on silicon. *Opt. Lett.* **31,** 2133–2135 (2006).
61. Verhagen, E., Spasenović, M., Polman, A. & Kuipers, L. K. Nanowire plasmon excitation by adiabatic mode transformation. *Phys. Rev. Lett.* **102,** 203904 (2009).
62. Dickson, R. M. & Lyon, L. A. Unidirectional plasmon propagation in metallic nanowires. *J. Phys. Chem. B* **104,** 6095–6098 (2000).
63. Ditlbacher, H. *et al.* Silver nanowires as surface plasmon resonators. *Phys. Rev. Lett.* **95,** 257403 (2005).
64. Sanders, A. W. *et al.* Observation of plasmon propagation, redirection, and fan-out in silver nanowires. *Nano Lett.* **6,** 1822–1826 (2006).
65. Wang, K. & Mittlemann, D. M. Metal wires for terahertz wave guiding. *Nature* **432,** 376–379 (2004).
66. Knight, M. W. *et al.* Nanoparticle-meditated coupling of light into a nanowire. *Nano Lett.* **7,** 2346–2350 (2007).
67. Pyayt, A. L., Wiley, B., Xia, Y., Chen, A. & Dalton, L. Integration of photonic and silver nanowire plasmonic waveguides. *Nature Nanotech.* **3,** 660–665 (2008).
68. Veronis, G. & Fan, S. Theoretical investigation of compact couplers between dielectric slab waveguides and two-dimensional metal–dielectric–metal plasmonic waveguides. *Opt. Express* **15,** 1211–1221 (2007).
79. Pile, D. F. P. & Gramotnev, D. K. Plasmonic subwavelength waveguides: Next to zero losses at sharp bends. *Opt. Lett.* **30,** 1186–1188 (2005).
70. Pile, D. F. P. & Gramotnev, D. K. Nanoscale Fabry–Pérot interferometer using channel plasmon-polaritons in triangular metallic grooves. *Appl. Phys. Lett.* **86,** 161101 (2005).
71. Volkov, V. S., Bozhevolnyi, S. I., Devaux, E., Laluet, J.-Y. & Ebbesen, T. W. in *Plasmonic Nanoguides and Circuits* (ed. Bozhevolnyi, S. I) 317–352 (Pan Stanford, 2009).
72. Søndergaard, T. & Bozhevolnyi, S. Slow-plasmon resonant nanostructures: Scattering and field enhancements. *Phys. Rev. B* **75,** 073402 (2007).
73. Miyazaki, H. T. & Kurokawa, Y. Squeezing visible light waves into a 3-nm-thick and 55-nm-long plasmon cavity. *Phys. Rev. Lett.* **96,** 097401 (2006).
74. Novotny, L. Effective wavelength scaling for optical antennas. *Phys. Rev. Lett.* **98,** 266802 (2007).

75. Bozhevolnyi, S. I. & Søndergaard, T. General properties of slow-plasmon resonant nanostructures: Nano-antennas and resonators. *Opt. Express* **15,** 10869–10877 (2007).
76. Lim, J. K., Imura, K., Nagahara, T., Kim, S. K. & Okamoto, H. Imaging and dispersion relations of surface plasmon modes in silver nanorods by near-field spectroscopy. *Chem. Phys. Lett.* **412,** 41–45 (2005).
77. Neubrech, F. *et al.* Resonances of individual metal nanowires in the infrared. *Appl. Phys. Lett.* **89,** 253104 (2006).
78. Allione, M., Temnov, V. V., Fedutik, Y., Woggon, U. & Artemyev, M. V. Surface plasmon mediated interference phenomena in low-*Q* silver nanowire cavities. *Nano Lett.* **8,** 31–35 (2008).
79. Miyazaki, H. T. & Kurokawa, Y. Controlled plasmon resonance in closed metal/insulator/metal nanocavities. *Appl. Phys. Lett.* **89,** 211126 (2006).
80. Søndergaard, T., Beermann, J., Boltasseva, A. & Bozhevolnyi, S. I. Slow-plasmon resonant-nanostrip antennas: Analysis and demonstration. *Phys. Rev. B* **77,** 115420 (2008).
81. Barnard, E. S., White, J. S., Chandran, A. & Brongersma, M. L. Spectral properties of plasmonic resonator antennas. *Opt. Express* **16,** 16529–16537 (2008).
82. Tang, L. *et al.* Nanometre-scale germanium photodetector enhanced by a near-infrared dipole antenna. *Nature Photon.* **2,** 226–229 (2008).
83. Bozhevolnyi, S. I. in *Nanophotonics with Surface Plasmons* (eds Shalaev, V. M. & Kawata, S.) 1–34 (Elsevier, 2007).
84. Sincerbox, G. T. & Gordon II, J. C. Small fast large-aperture light modulator using attenuated total reflection. *Appl. Opt.* **20,** 1491–1494 (1981).
85. Solgaard, O., Ho., F., Thackara, J. I. & Bloom, D. M. High frequency attenuated total internal reflection light modulator. *Appl. Phys. Lett.* **61,** 2500–2502 (1992).
86. Dicken, M. J. *et al.* Electrooptic modulation in thin film barium titanate plasmonic interferometers. *Nano Lett.* **8,** 4048–4052 (2008).
87. Dionne, J. A., Diest, K., Sweatlock, L. A. & Atwater, H. A. PlasMOStor: A metal-oxide–Si field effect plasmonic modulator. *Nano Lett.* **9,** 897–902 (2009).
88. MacDonald, K. F., Sámson, Z. L., Stockman, M. I. & Zheludev, N. I. Ultrafast active plasmonics. *Nature Photon.* **3,** 55–58 (2009).
89. Pacifici, D., Lezec, H. J. & Atwater, H. A. All-optical modulation by plasmonic excitation of CdSe quantum dots. *Nature Photon.* **1,** 402–406 (2007).
90. Pala, R. A., Shimizu, K. T., Melosh, N. A. & Brongersma, M. L. A nonvolatile plasmonic switch employing photochromic molecules. *Nano Lett.* **8,** 1506–1510 (2008).
91. Sudarkin, A. N. & Demkovich, P. A. Excitation of surface electromagnetic waves on the boundary of a metal with an amplifying medium. *Sov. Phys. Tech. Phys.* **34,** 764–766 (1989).
92. Sirtori, C. *et al.* Long-wavelength ($\lambda \approx 8$–11.5 μm) semiconductor lasers with waveguides based on surface plasmons. *Opt. Lett.* **23,** 1366–1368 (1998).
93. Tredicucci, T. *et al.* Single-mode surface-plasmon laser. *Appl. Phys. Lett.* **76,** 2164–2166 (2000).
94. Seidel, J., Grafström, S. & Eng, L. Stimulated emission of surface plasmons at the interface between a silver film and an optically pumped dye solution. *Phys. Rev. Lett.* **94,** 177401 (2005).
95. Noginov, M. A. *et al.* Compensation of loss in propagating surface plasmon polaritons by gain in adjacent dielectric medium. *Opt. Express* **16,** 1385–1392 (2008).
96. Ambati, M. *et al.* Observation of stimulated emission of surface plasmon polaritons. *Nano Lett.* **8,** 3998–4001 (2008).
97. Grandidier, J. *et al.* Gain-assisted propagation in a plasmonic waveguide at telecom wavelength. *Nano Lett.* **9,** 2935–2939 (2009).
98. Noginov, M. A. *et al.* Stimulated emission of surface plasmon polaritons. *Phys. Rev. Lett.* **101,** 226806 (2008).
99. van Wijngaarden, J. T. *et al.* Direct imaging of propagation and damping of near-resonance surface plasmon polaritons using cathodoluminescence spectroscopy. *Appl. Phys. Lett.* **88,** 221111 (2006).
100. Bashevoy, M. V., Jonsson, F., Krasavin, A. V. & Zheludev, N. I. Generation of traveling surface plasmon waves by free-electron impact. *Nano Lett.* **6,** 1113–1115 (2006).
101. Koller, D. M. *et al.* Organic plasmon-emitting diode. *Nature Photon.* **2,** 684–687 (2008).
102. Chang, D. E., Sørensen, A. S., Hemmer, P. R. & Lukin, M. D. Quantum optics with surface plasmons. *Phys. Rev. Lett.* **97,** 053002 (2006).
103. Chang, D. E., Sørensen, A. S., Hemmer, P. R. & Lukin, M. D. Strong coupling of single emitters to surface plasmons. *Phys. Rev. B* **76,** 035420 (2007).
104. Jun, Y. C., Kekatpure, R. D., White, J. S. & Brongersma, M. L. Nonresonant enhancement of spontaneous emission in metal–dielectric–metal plasmon waveguide structures. *Phys. Rev. B* **78,** 153111 (2008).
105. Fedutik, Y., Temnov, V. V., Schöps, O., Woggon, U. & Artemyev, M. V. Excitation–plasmon–photon conversion in plasmonic nanostructures. *Phys. Rev. Lett.* **99,** 136802 (2007).
106. Akimov, A. V. *et al.* Generation of single optical plasmons in metallic nanowires coupled to quantum dots. *Nature* **450,** 402–406 (2007).
107. Chang, D. E., Sørensen, A. S., Demler, E. A. & Lukin, M. D. A single-photon transistor using nanoscale surface plasmons. *Nature Phys.* **3,** 807–812 (2007).
108. Ditlbacher, H. *et al.* Organic diodes as monolithically integrated surface plasmon polariton detectors. *Appl. Phys. Lett.* **89,** 161101 (2006).
109. Neutens, P. *et al.* Electrical detection of confined gap plasmons in metal–insulator–metal waveguides. *Nature Photon.* **3,** 283–286 (2009).
110. Falk, A. L. *et al.* Near-field electrical detection of optical plasmons and single-plasmon sources. *Nature Phys.* **5,** 475–479 (2009).
111. Lal, S., Link, S. & Halas, N. J. Nano-optics from sensing to waveguiding. *Nature Photon.* **1,** 641–648 (2007).
112. Genet, C. & Ebbesen, T. W. Light in tiny holes. *Nature* **445,** 39–46 (2007).
113. Challener, W. A. *et al.* Heat-assisted magnetic recording by a near-field transducer with efficient optical energy transfer. *Nature Photon.* **3,** 220–224 (2009).
114. Noginov, M. A. *et al.* Demonstration of a spaser-based nanolaser. *Nature* **460,** 1110–1112 (2009).
115. Oulton, R. F. *et al.* Plasmon lasers at deep subwavelength scale. *Nature* **461,** 629–632 (2009).
116. Volkov, V. S., Bozhevolnyi, S. I., Devaux, E. & Ebbesen, T. W. Bend loss for channel plasmon polaritons. *Appl. Phys. Lett.* **89,** 143108 (2006).

Acknowledgements

This work was partially supported by the Danish Agency for Science, Technology and Innovation grant No. 274-07-0258 (SIB), and by the Australian Research Council, Australian Federal Police and National Institute of Forensic Science (ARC Linkage Grant No: LP0882614).

Additional information

The authors declare no competing financial interests.